

Regularity of cochlear nucleus stellate cells: A computational modeling study

Michael J. Hewitt and Ray Meddis

Speech and Hearing Laboratory, Department of Human Sciences, University of Technology, Loughborough, LE11 3TU, United Kingdom

(Received 11 August 1992; accepted for publication 1 March 1993)

This article reports on a computational modeling study designed to investigate the generation of the transient chopper response of cochlear nucleus stellate cells. The model is based on a simulation of the auditory periphery which feeds a generic stellate-cell model. Physiological recordings of transient chopper units in response to short, best frequency, tone bursts show a brief initial period (typically < 10 ms) of rapid rate adaptation as evidenced by a rapid rise in mean interspike interval. Associated with this rate adaptation is a significant increase in firing irregularity. The changes in rate and irregularity have recently been attributed to the activation of noisy inhibitory inputs on the cell [e.g., Banks and Sachs, *J. Neurophysiol.* **65**, 606–629 (1991)]. However, the results show that the transient chopper response pattern can be generated without the need for inhibitory inputs. The transience of the initial chopping pattern is sensitive to the following model parameters: (a) the firing threshold of the cell, (b) the number of excitatory inputs that converge on the cell, and (c) the magnitude of the current delivered to the cell for each active input. The response was also found to be relatively insensitive to changes in the degree of dendritic filtering imposed on the auditory-nerve input. The results of each simulation can be explained by considering the pattern of depolarization the cell receives during the course of a tone burst.

PACS numbers: 43.64.Qh, 43.64.Bt

INTRODUCTION

One goal of contemporary auditory neuroscience is to explain the mechanisms which generate the varied response patterns shown by different types of cochlear-nucleus neurons. Considerable progress in the field has been made in recent years using intracellular recording techniques and brain slice preparations (see Young *et al.*, 1988b; Rhode and Greenberg, 1992, for a review). In parallel, computer models have provided a framework within which data from anatomical and physiological studies can be drawn together into comprehensive and testable theories. This paper reports on a computational modeling study designed to investigate the generation of the transient chopper response pattern.

In physiological studies of the cochlear nucleus, the chopper response pattern is commonly observed. A chopper poststimulus time histogram (PSTH) is characterized by a series of regularly spaced peaks of neural discharge which become less distinct after about 20 ms (Pfeiffer, 1966). The rate of chopping is, in general, unrelated to the stimulus frequency. The chopper response pattern is commonly associated with stellate (or multipolar) cells found in the anterior and posterior regions of the ventral cochlear nucleus (VCN) (Rhode *et al.*, 1983; Rouiller and Ryugo, 1984; Smith and Rhode, 1989). The population of chopper units is not, however, homogeneous but instead consists of a number of subgroups.

One technique commonly used to distinguish chopper subgroups is that of regularity analysis (Young *et al.*, 1988a). The procedure yields the coefficient of variation

(CV) metric (defined below) which is a measure of the regularity of a neuron's firing pattern over the duration of short (< 50 ms), best-frequency (BF) tone bursts. On the basis of the CV metric, cells may be grouped into one of two main categories, examples of which are presented in Fig. 1. Regular or sustained choppers (chop-S) have low CVs (< 0.3) which remain relatively constant over the duration of the tone burst. Irregular choppers have CVs that rapidly increase over the first 10–15 ms of response (e.g., CV < 0.3 at onset and CV > 0.3 at $t = 15$ ms) and then plateau (Young *et al.*, 1988a; Blackburn and Sachs, 1989). This latter response pattern is exhibited by two physiologically distinct units found within the ventral cochlear nucleus. These are the transient choppers (chop-T cells) and the onset choppers (O_c cells).

Blackburn and Sachs (1989) propose that the transient chopper response pattern can be explained in terms of a period of initial excitation which produces regular firing, followed by a combination of excitation and inhibition which produces a less regular firing pattern. The theory further speculates that sustained chopper cells receive considerably less inhibition than the transient chopper cells; accordingly the sustained chopper firing pattern represents the uninhibited response of stellate cells.

A recent modeling study has shown that the theory is tenable. Banks and Sachs (1991) produced a generic model of VCN chopper units. The model consisted of an equivalent cylinder compartmental model to simulate cell dendrites together with a model cell soma based on the Hodgkin and Huxley equations of spike-generation. Input to the model was modeled as a deadtime-modified Poisson

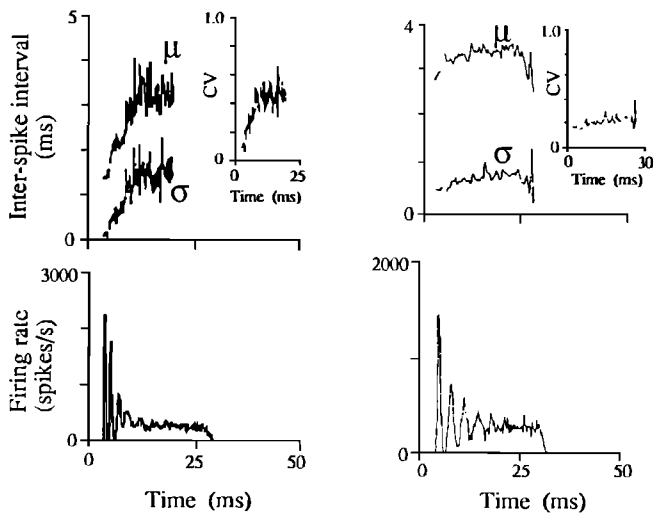


FIG. 1. Regularity analysis data and PSTHs from a transient chopper (left column) and a sustained chopper (right column). Input level 30 dB above threshold. In the regularity plots, μ is the mean interspike interval, σ is the standard deviation of interspike intervals, and CV is the ratio σ/μ . Adapted from Young *et al.* (1988a, Figs. 4B and 2B).

process with two-component adaptation in the Poisson rate.

Banks and Sachs systematically varied the number, rate, and location of excitatory and inhibitory inputs to the model. They quantified the regularity of the model's response with the coefficient of variation metric. One of their main findings was that the model could only produce realistic transient chopper response patterns when simulated inhibitory inputs were activated.

In another modeling study, Arle and Kim (1991) generated realistic sustained and transient chopper responses from a generic cell-soma model. Input to the model was in the form of step currents modulated with Gaussian noise. The rationale of the approach was to formulate hypotheses regarding the nature of the current that must exist at the cell soma during pure-tone stimulation in order to generate the different chopper response patterns.

To generate a transient chopper response pattern the current at the soma needed to show an increased degree of irregularity during the time course of the stimulus, whereas, the sustained chopper pattern could be generated from a steady average current level with relatively small variability. Arle and Kim (1991) suggest that the irregular current profile required for the transient chopper response pattern could result from the activation of inhibitory inputs.

Given these data, the inhibition hypothesis seems a likely explanation for the transient chopper response. It is also possible, however, that inhibition need not be the only mechanism that operates within stellate cells to produce the transient chopper response. Other mechanisms in conjunction with inhibition may account for the response. Evidence to support this conjecture is demonstrated by intracellular recordings of stellate cells. Smith and Rhode (1989, Fig. 4) show stellate cells with an irregular response patterns despite the fact that high levels of sustained depo-

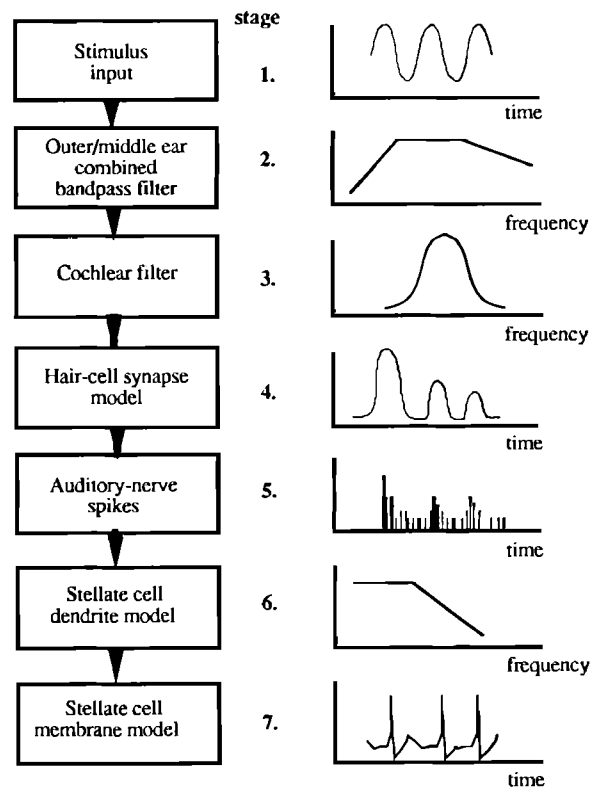


FIG. 2. Model processing sequence (see text for details).

larization were observed throughout the duration of a tone burst. Similar findings have been reported by Romand (1978; 1979).

Additionally, Smith and Rhode (1989, Fig. 3) show intracellular records from sustained choppers which display apparent inhibitory potentials. These inhibitory potentials were observed for stimulus frequencies above and below cell best frequency and, at the offset of best frequency tone bursts. No inhibitory potentials were observed from similar recordings from stellate cells which showed a transient chopper response. Such evidence is hard to reconcile with a theory based upon inhibition per se.

Smith and Rhode (1989) discuss a number of other mechanisms that may account for the transient chopper response. For example, they suggest that the threshold of firing in the (irregular firing) onset-chopper cells could be higher than that of the (regular firing) chop-S cells. Cells with relatively high firing thresholds can only be driven in a (regular) chop-S-like fashion when the summed effects of the converging auditory-nerve inputs are maximal. This condition occurs at the onset of the auditory-nerve response to stimuli and declines thereafter due to adaptation.

The purpose of this paper is to show, using computer simulation techniques, that a sustained chopper pattern can be made transient without the activation of inhibitory inputs. The change from sustained to transient output can be explained by considering the pattern of depolarization induced in a cell relative to its threshold during the course of a tone burst. We show that a number of intercell differences, such as variation in cell firing threshold, may influence the pattern of output from stellate cells.

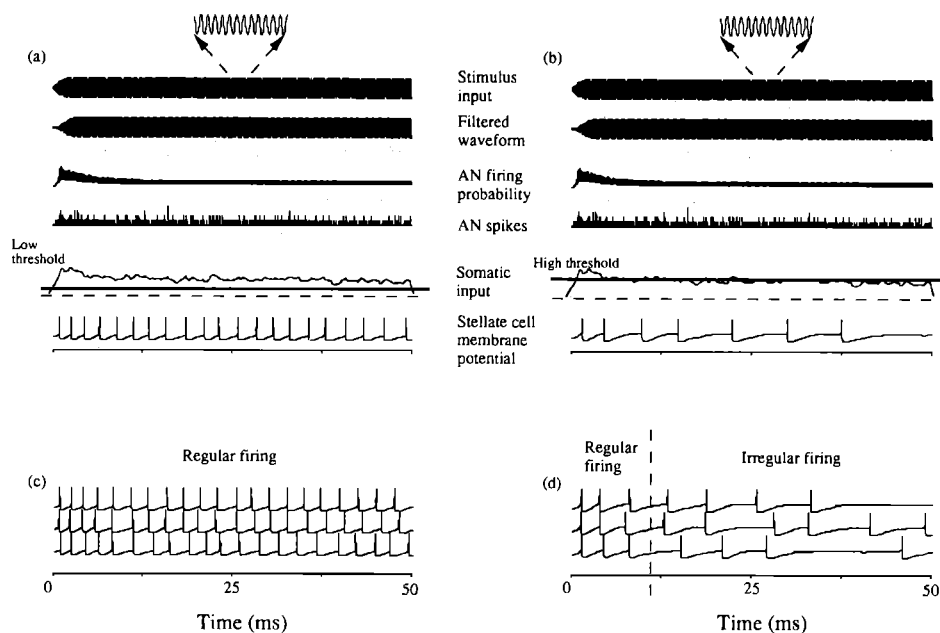


FIG. 3. Example model output. Simulations (a) and (b) each receive as input a 5-kHz tone burst. The tone burst is processed by a model of the auditory periphery which includes linear bandpass filtering and mechanical to neural transduction. The output of the peripheral model "AN spikes" is low-pass filtered which forms the input to the point-neuron model ("somatic input"). In (a), the model stellate cell has a relatively low threshold of firing (thick line drawn across "somatic input"). The somatic input is sufficiently high to elicit spikes of regular intervals throughout the duration of the tone burst. In (b), the model has a relatively high threshold of firing. The somatic current is only sufficiently strong to drive the cell in a regular fashion during the first 10–12 ms of the stimulus. In (c) and (d) model outputs are shown from three consecutive stimulus presentations. Model parameters: $N=60$, $\Delta I=0.2$ nA, $f_c=300$ Hz.

I. METHODS

A. Model description

The stages of the composite model are shown schematically in Fig. 2 and are summarized below. Details of the peripheral auditory model can be found in previous publications (e.g., Meddis and Hewitt, 1991). The equations that describe the stellate-cell model are presented in the Appendix. Examples of model output from the main processing stages are shown in Fig. 3.

(1) Stimulus input. Except where explicitly stated, signals are 5-kHz sine wave tone bursts of 50-ms duration with 5-ms rise time. Stimulus presentation level was always 30 dB above the stellate-cell model's reference level (defined below).

(2) Outer-ear/middle-ear combined bandpass filter. Negligible changes are imposed on a 5-kHz tone burst by this stage of the model.

(3) Cochlear filter to simulate the mechanical filtering action of the basilar membrane. This was implemented using a single linear bandpass digital filter based on the gamma-tone function (Patterson *et al.*, 1988). The required channel is specified by its center frequency. Unless stated otherwise, the center frequency of the channel was 5 kHz. The 3-dB bandwidth of the 5-kHz filter is 577 Hz (Patterson *et al.*, 1988). Figure 3 shows the output of a gamma-tone filter ("filtered waveform") centered on 5 kHz in response to a 5-kHz tone burst. Negligible changes are imposed on the input waveform by this stage of the model.

(4) Mechanical to neural transduction at the inner-

hair cell/auditory-nerve synapse. This was implemented using the computer model proposed by Meddis (1986, 1988; Meddis *et al.*, 1990). The output of this stage is expressed as the probability of occurrence of a spike in an auditory-nerve (AN) fiber of the 5-kHz channel ("AN firing probability," Fig. 3).

The simulation of the inner hair cell/AN junction imposes several changes on the waveform. The most significant change is the adaptation of response. Auditory nerve fiber adaptation has been quantified as the sum of two exponential decay constants. Rapid adaptation has a time constant of under 10 ms and short-term adaptation has a time constant of about 40 ms (Westerman and Smith, 1984). The model of the hair-cell/AN junction used in this study replicates this behavior accurately (Meddis, 1988; Hewitt and Meddis, 1991).

The parameters of the hair-cell model were set to simulate a fiber with a spontaneous rate of about 35 spikes/s, a saturated rate of about 150 spikes/s and a limited (30 dB) dynamic range (Hewitt *et al.*, 1992).

(5) Auditory nerve spike generation and refractory effects. Refractory inhibition of firing of the auditory-nerve was computed as an adjustment to the hair cell firing probability as a function of time since it last generated a spike (see Meddis and Hewitt, 1991 for details).

Individual AN spikes were generated from the hair-cell firing probability using pseudorandom number techniques (e.g., Hastings and Peacock, 1975, p. 41). Simulated AN spikes generated by this method yields nonstationary Poisson processes modified by a deadtime

TABLE I. Stellate cell model parameters (see Appendix for definitions). The parameters varied in the study are marked with an asterisk (ranges shown in brackets).

Parameter	Value/Range
c	0.3
τ_{TH}	20.0 ms
b	0.017
τ_{Gk}	0.35 ms
τ_m	2.0 ms
R_i	33.0 M Ω
E_b	50.0 mV
E_R	-60.0 mV
E_k	-10.0 mV
* Th_0	(5-15 mV)
* N	(30-120)
* ΔI	(0.14-0.25 nA)
* f_c	(300-5000 Hz)

(Young and Barta, 1986). Due to the probabilistic nature of the technique, a different pattern of auditory-nerve spikes is delivered to the model stellate cell on each stimulus presentation. The output of this stage represents the number of active auditory-nerve fibers per time unit simulated ("AN spikes", Fig. 3). Unless stated otherwise, 60 auditory-nerve fiber inputs were simulated.

(6) Dendrite model. The train of AN spikes is low-pass filtered to simulate dendritic filtering. The filter was implemented as a first-order low-pass digital filter to give 6-dB attenuation per octave. Unless stated otherwise, the filter cutoff frequency was set to 300 Hz. The main consequence of low-pass filtering is that the auditory-nerve input is smeared over time. The effects of a spike are not simply instantaneous, but continue to influence the cell membrane for some time after ("somatic input," Fig. 3).

This simple model of stellate-cell dendrites was implemented to reduce computation time. However, the model produces simulated excitatory potentials that closely mimic those recorded empirically by Oertel (1985) from stellate cells maintained *in vitro* (see Hewitt *et al.*, 1992 for details).

(7) The cell-membrane model was a simplified model of the Hodgkin and Huxley equations of spike generation (MacGregor, 1987). The differential equations describing the model are presented in the Appendix.

The sequences of waveforms shown in Fig. 3 represent one pass through the model (i.e., one stimulus presentation). Figure 3(a) shows model output where the threshold of firing was 5 mV and Fig. 3(b) shows model output where the threshold of firing was 15 mV.

The input to the cell-membrane model is the filtered AN spikes ("somatic input"). The simulated dendritic filtering does not remove the temporal adaptation characteristics imposed on the signal by the hair-cell synapse. In fact, average somatic current declines as a function of signal duration, with most adaptation taking place within the first 10 ms of response.

In Fig. 3(b) the interspike interval lengthens as adaptation of the input takes place whereas in Fig. 3(a) the cell potential is well above firing threshold and maintains a

fairly constant interspike interval (dictated mainly by the recovery time of the neuron) despite adaptation.

Associated with the differences in interspike intervals, there are differences in the *precise* timing of spikes from one stimulus presentation to the next. This is illustrated in Fig. 3(c) and (d) which shows outputs from three consecutive stimulus presentations. For the low-threshold model [Fig. 3(c)] the precise timing of spikes is almost invariant from one stimulus presentation to the next. In contrast, for the high threshold model [Fig. 3(d)] such precision is maintained for only a short period following stimulus onset. These and other model outputs may be quantified using the technique known as regularity analysis.

B. Regularity analysis

One of the most sensitive and reliable techniques used to apportion chopper units into subgroups is that of regularity analysis (Young *et al.*, 1988a). The technique involves calculating the mean and standard deviation of interspike intervals (μ_R and σ_R , respectively) as a function of the time of occurrence of the first spike in the interval. For a given spike train, interspike intervals are computed and the interval values are placed in time bins according to the latency of the first spike in the interval. A histogram of interval values is built up over a large number of stimulus repetitions. The mean and standard deviation of interspike intervals within each time bin are calculated as

$$\mu_{R_j} = \frac{1}{N_j} \sum_{i=1}^{N_j} I_{ij}, \quad (1)$$

where N_j is the number of intervals in the j th histogram bin and I_{ij} is the duration of each interval where the first spike of the interval fell in the j th bin (spike latency = $j \cdot \Delta$, where Δ is the histogram bin width):

$$\sigma_{R_j}^2 = \frac{1}{(N_j - 1)} \sum_{i=1}^{N_j} (I_{ij} - \mu_{R_j})^2. \quad (2)$$

The coefficient of variance ($CV = \sigma_R / \mu_R$) quantifies the regularity of a cell's output, with a low CV value indicating regularity.¹

Mean and standard deviation of interspike intervals together with CV values are calculated from model responses to 500 repetitions of a short, best frequency tone (5 kHz). A tone duration of 50 ms is used, though the calculations are terminated at 25 ms to avoid end effects, as discussed in Young *et al.* (1988a). The histogram bins are 0.2 ms wide. All plots except the PSTHs are smoothed with a 3-bin-wide triangular filter, and bins are only plotted if they contain three or more spikes. Following the methods of Blackburn and Sachs (1989), average CV is calculated between 15- and 20-ms post-stimulus onset.

The input level of the tone is always 30 dB above the model's reference level (0 dB). Following the methods of Hewitt *et al.* (1992) 0 dB is defined as the level at which the stellate-cell model's onset and steady-state rate-level functions start to diverge.

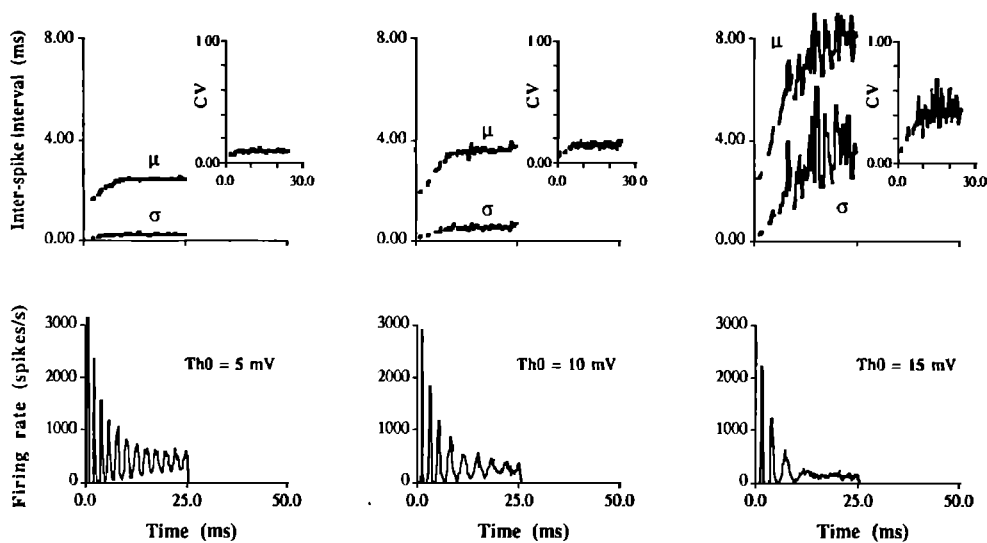


FIG. 4. Regularity analysis and PSTHs from model stellate cell with different firing thresholds. Average CVs are 0.09, 0.14, and 0.46 for $Th_0=5, 10,$ and 15 mV, respectively. Other model parameters: $N=60, \Delta I=0.2$ nA, $f_c=300$ Hz.

Physiologists only include units in their chopper population if a spike contributes to each well-defined chopping peak on every stimulus presentation (see Young *et al.*, 1988a for details). Blackburn and Sachs (1989) limited this criteria to apply to only the first two chopping peaks of a PSTH. They classified units as choppers only if the “spikes per peak” measures for the first two chopping peaks were 0.95–1.05 and 0.92–1.05, respectively. That is, the first two spikes in each spike train almost always contributed to the first two peaks in the chopping PSTH. All simulations reported here satisfied these criteria.

II. MODEL EVALUATION

In the simulations several parameters of the model are held constant. These are listed in Table I. We systemati-

cally vary other model parameters (ranges shown in Table I) and record the changes in the regularity of the model’s output.

A. Firing threshold

We are able to model differences in cell firing threshold by changing the model parameter, Th_0 . This parameter largely determines the cell potential required before a spike (or action potential) is generated. We first investigate the effects of variations in the model firing threshold on the regularity of it’s output. Values of $Th_0=5, 10,$ and 15 mV were used.

As the threshold of firing increases, three main changes in the response of the model are apparent (Fig. 4). First, there is increased rate adaptation as evidenced by the increase in the mean interspike interval. Accompanied by

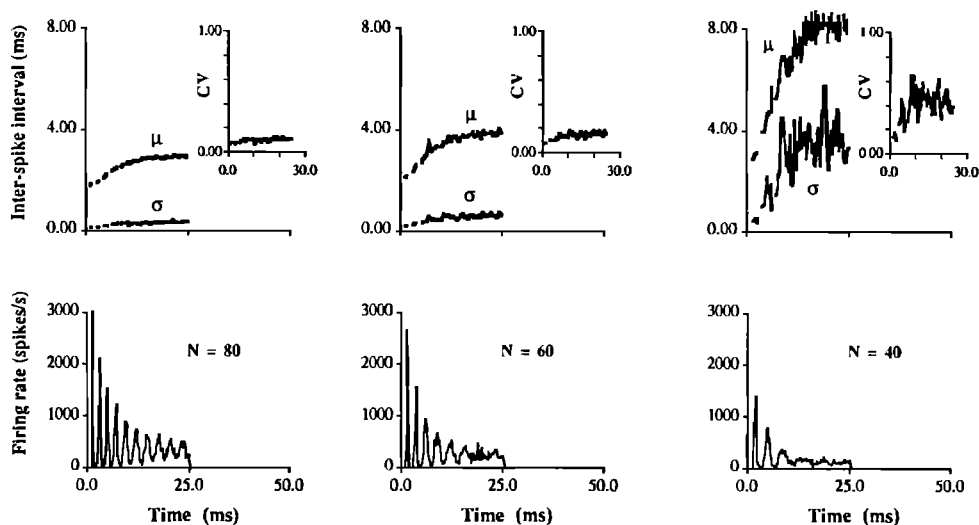


FIG. 5. Regularity analysis and PSTHs from model stellate cell with different N (number of inputs). Average CVs are 0.1, 0.15, and 0.45 for $N=80, 60,$ and 40, respectively. Other model parameters: $Th_0=10.0, \Delta I=0.2$ nA, $f_c=300$ Hz.

the increased rate adaptation is a rise in irregularity as evidenced by the increase in average CV. Finally, there is an increased transience of the initial chopping response; with $Th_0=5$ mV and $Th_0=10$ mV the model responses are typical of sustained chopper units, and with $Th_0=15$ mV the response is typical of a transient chopper unit.

One quantitative difference between the transient-chopper model ($Th_0=15$ mV) and neural data concerns the size of the mean and standard deviation of interspike intervals. For the period 15- to 20-ms post-stimulus onset, the mean interval (μ_R) and standard deviation (σ_R) statistics are about 2.5 and 0.5 ms greater, respectively, than the corresponding neural data shown in Fig. 1. However, units with interval statistics similar to those of the model were present in Young *et al.*'s (1988a) sample as shown in their Fig. 7. We shall return to this issue later. The results show, however, that a model displaying a sustained chopper pattern can be changed to a transient chopper pattern simply by raising its firing threshold.

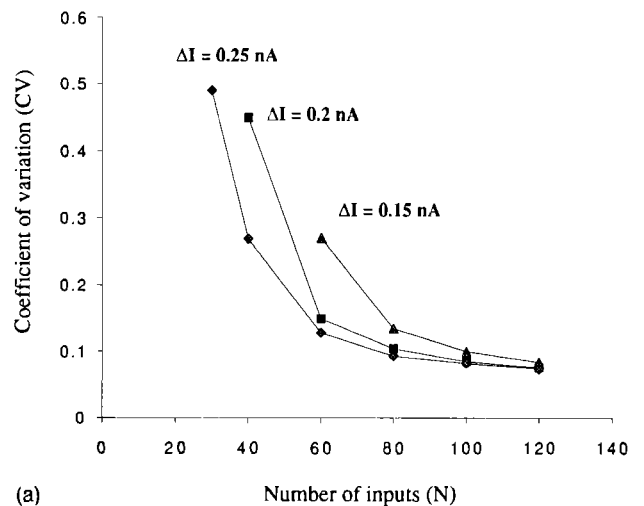
B. The number of auditory nerve fiber inputs

Anatomical studies have differentiated between two types of stellate cells in the cochlear nucleus based on the location of the primary input to the cells (Cant, 1981; Cant and Morest, 1984). Type I stellate cells have somata that are only sparsely covered with synaptic terminals and receive most of their input on their dendritic trees. Type II cells receive the majority of input via synaptic terminals on their somata and are only sparsely innervated on their dendritic trees. It is not known how many AN fibers contact a single stellate cell. However, these findings make it likely that the number of inputs to the two different cell types may differ markedly.

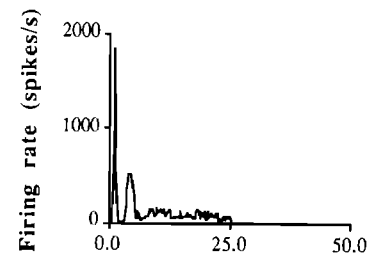
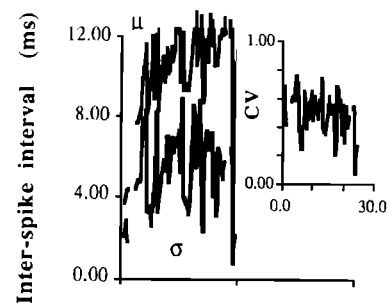
In Hewitt *et al.* (1992) the total amount of current that could be delivered to the cell I_{max} was fixed while the number of inputs to the cell N was variable. The current delivered to the cell per active input ΔI was simply determined by dividing I_{max} by N . The assumption that each cell in a population of cells is capable of receiving the same total current was convenient but at the same time unrealistic. In this study, therefore, we decided to vary the number of inputs to the cell N but hold constant the current per active input ($\Delta I=0.2$ nA).²

Figure 5 shows model regularity data and PSTHs for $N=80, 60,$ and 40 . Between 60 and 40 inputs, the response pattern changes from sustained to transient. With 40 inputs there is a brief period of rapid rate adaptation and a marked increase in irregularity during the first 10 ms of response. This response is typical of transient choppers.

Figure 6(a) shows average CV as a function of the number of inputs and for different values of current per active unit. The change from relatively high CV to relatively low CV occurs between 60 and 40 inputs. No data are presented for the combination $\Delta I=0.15, N < 60$ or for $\Delta I=0.2, N < 40$. In these cases the model post-stimulus time histograms no longer resemble those of sustained or transient chopper units [e.g., Fig. 6(b)]. Such a unit would be classified as chop-U (Young *et al.*, 1988a). Chop-U or unusual units are not recognized as a separate class of



(a)



(b)

FIG. 6. (a) Average CV (15–20 ms post-stimulus onset) from model stellate cell as a function of N (number of inputs) and for different values of ΔI . (b) Regularity data and PSTH from model stellate cell with chop-U characteristics. Average CV is 0.5. Parameters: $N=30, \Delta I=0.2$ nA, $f_c=300$ Hz.

choppers but instead are thought to be closely related to a group of units known as primary-like with notch (Young *et al.*, 1988a).

C. Input current magnitude

The amount of post-synaptic current delivered by an auditory nerve action potential is unknown. However, the current strength parameter ΔI should be as influential as the number of inputs in determining the response type of the cell. We investigate this by holding constant the number of inputs ($N=60$), and varying the current per active input ΔI . Values of $\Delta I=0.2, 0.17,$ and 0.14 nA per action potential were used. As the variable parameter ΔI is reduced (Fig. 7), the response pattern changes from sustained to transient.

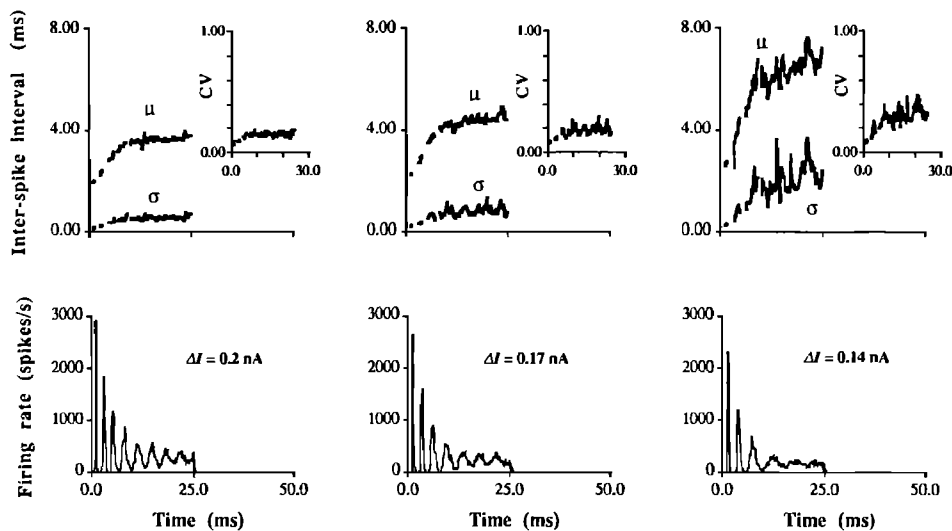


FIG. 7. Regularity analysis and PSTHs from model stellate cell with different input magnitudes. Average CVs are 0.14, 0.19, and 0.31 for input magnitudes of 0.2, 0.17, and 0.14 nA, respectively. Other model parameters: $\text{Th}_0 = 10$, $N = 60$, $f_c = 300$ Hz.

D. Dendritic filtering

Stellate cells have been grouped into one of two types based on whether the synaptic connections to the cell are predominantly somatic or dendritic (e.g., Cant, 1981). These distinguishing features may have important implications for the transmission of the input signal as it travels from the synapse to the site of spike initiation on the cell soma.

If it is assumed that the spread of current down a dendrite to the soma is a passive process then the signal at the soma will be attenuated compared to the signal at the dendrite. Application of cable theory (e.g., Rall, 1989) predicts that the signal at the soma is a low-pass filtered version of the input signal. The effects of the filtering become increasingly significant as the distance increases between the synaptic contact and soma.

The effects of simulated dendritic filtering on the model's output were investigated by comparing six possible cut-off frequencies f_c of the low-pass filter in the range 300–5000 Hz. The choice of the lowest value of $f_c = 300$ Hz was determined from data presented in Hewitt *et al.* (1992). Briefly, this value gave a good quantitative fit to chopper synchronization data. A lower value produced model results that tended to underestimate the cutoff frequency of chopper phase locking. A filter cutoff frequency of 5 kHz simulates only very limited dendritic filtering and the input to the soma closely resembles that of the original AN input.

Figure 8 shows model CV values as a function of f_c and for different values of model firing threshold Th_0 . Changing f_c had almost no effect on model CV for cell firing thresholds of 5 and 10 mV. In all these conditions, the model produced typical sustained chopper post-stimulus time histograms. Transient chopper response patterns and average CVs > 0.3 were obtained with a cell firing threshold of 15 mV. For this condition, average CV falls as f_c increases. A closer inspection of these results shows that an increase in f_c leads to a small, but significant, rise in the

model's firing rate. This results in a reduced value of the mean interspike interval (μ_R) which automatically sets a lower ceiling on the maximum CV.¹

E. Other model parameters

Within each population of VCN chopper units there is a range of mean interspike interval data. For sustained and transient chopper units mean interval values fall between about 1.6 and 8 ms (e.g., Young *et al.*, 1988a, Fig. 7). The model data presented in Figs. 4, 5, and 7 have shown sustained choppers with relatively short mean intervals (e.g., 3–4 ms) and transient choppers with relatively long mean intervals (e.g., 7–8 ms). Previous work (Hewitt *et al.*, 1992) has shown that the model interspike interval is sensitive to a number of independently varied parameters. These include the parameters that govern the magnitude and duration of the potassium conductance (b, τ_{GK}) and

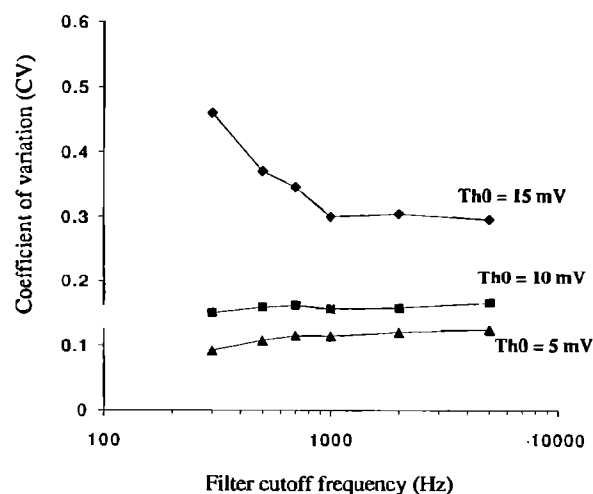


FIG. 8. Average model CV (15–20 ms post-stimulus onset) plotted as a function of the low-pass filter cutoff frequency f_c and for different cell thresholds Th_0 . Other model parameters: $N = 60$, $\Delta I = 0.2$ nA.

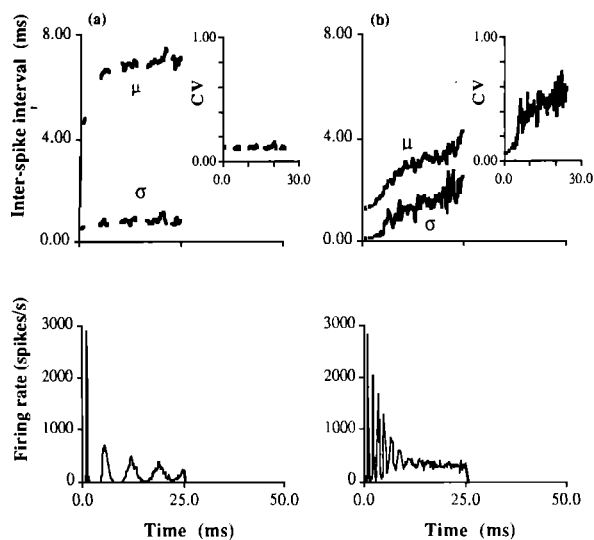


FIG. 9. Regularity data and PSTHs from model stellate cell with different membrane properties and firing thresholds. (a) Simulation of a sustained chopper unit with mean interspike interval of 6.9 ms. Parameters: $Th_0 = 10$ mV, $N = 60$, $\Delta I = 0.2$ nA, $f_c = 300$ Hz, $\tau_{Gk} = 0.0015$ s, $\tau_m = 0.002$ s. (b) Simulation of a transient chopper unit with a mean interspike interval of 3.2 ms. Parameters: $Th_0 = 15$ mV, $N = 60$, $\Delta I = 0.2$ nA, $f_c = 300$ Hz, $\tau_{Gk} = 0.0002$ s, $\tau_m = 0.0005$ s.

the membrane time constant (τ_m). Systematic variation of these parameters allows us to generate both sustained and transient response patterns with a range of interspike intervals. Two examples are shown in Fig. 9. Figure 9(a) shows a sustained chopper response pattern with a mean interspike interval of 6.9 ms. Figure 9(b) shows a transient chopper response pattern with a mean interval of 3.2 ms.

III. DISCUSSION

We have demonstrated that a transient chopper response pattern can be generated from a model of a VCN stellate cell without the activation of simulated inhibitory input.

A. Mechanism

When stellate-cell units are driven steadily above threshold by sufficiently high current levels they fire action potentials at an intrinsically determined rate. Moreover, the *precise* timing of each action potential is relatively invariant from one stimulus presentation to the next. The mechanism of regular firing has been ascribed to specific electrical characteristics of the membrane (e.g., Young *et al.*, 1988b). At lower current levels, the firing rate decreases and the timing of each action potential varies in successive stimulus presentations. These responses are apparent from *in vitro* preparations where stellate cells are injected with known magnitudes of current (Oertel *et al.*, 1988), and from *in vivo* preparations where regularity of response is measured as a function of sound-pressure level (Young *et al.*, 1988a).

It is possible to explain the modeling results presented in Figs. 4 to 7 in similar terms. If the somatic current is sufficiently high to drive the firing mechanism at its intrinsic

rate and maintain the precision of timing of each spike from trial to trial then a sustained chopper response pattern results. If the input current falls, such that it fluctuates above and below that required to maintain regularity, then a transient response pattern results (see Fig. 3).

Previously published research (Arle and Kim, 1991; Banks and Sachs, 1991) has shown that delayed inhibition could reduce input current to stellate cells and so produce a transient chopper response. Our results show that adaptation of the pure excitatory input to stellate cells can also produce the same response. Both mechanisms lead to the situation where, after the first 10 or so milliseconds of response, the driving potential delivered to the cells is reduced. In such cases, the intrinsic firing which dominates the early phase of the response is lost, the mean firing rate decreases and the output pattern is determined by the random fluctuations of the input profile.

The variation of firing threshold is only one of many possible model parameters that controls the regular/irregular output pattern. In terms of a chopper cell population, the model predicts that intercell differences such as threshold, number of inputs, or magnitude of input could all determine the type of response pattern observed.

The model enables us to consolidate our knowledge of stellate cell behavior as well as make some novel predictions. Following Smith and Rhode's (1989) suggestion our first simulation considered the effects of variation in cell firing threshold. Evidence that transient chopper cells have higher thresholds (either in dB SPL or in mV depolarization) than sustained chopper cells comes from two sources. Blackburn and Sachs (1990) show rate-level functions from six chopper units, three sustained chopper units and three transient chopper units. In all cases, the thresholds of the transient chopper units are about 10–20 dB higher than those of the sustained chopper units. Smith and Rhode (1989) show intracellular data from one sustained and one transient unit. The transient chopper unit had a higher threshold of membrane depolarization than the sustained chopper unit.

The model predicts that the regularity of stellate cell units may increase with increases in stimulus input level. In Fig. 3(b) for example it could be envisaged that an increase in stimulus level could drive the somatic input to a steady level above firing threshold and so produce regular firing. Data presented by Smith and Rhode (1989, Figs. 2D and 2E) lends support to this prediction. They show mean interval data for an onset chopper unit for stimulus levels of 50 and 70 dB above threshold. At 50 dB above rate threshold the unit shows an abrupt increase in mean interval corresponding to the transition from onset peaks to the sustained portion of the post-stimulus time histogram. At 70 dB the activity during the sustained portion of the unit's response is so robust that the mean interval data resembles those of sustained choppers.

One factor that seems to have only a limited influence on the regularity of model output is the degree of simulated dendritic filtering. It has been proposed that the regularity/irregularity of cells could be predicted by differences in the location of the primary input to different units

(e.g., Young *et al.*, 1988a). Stellate cells may be classified into one of two anatomically defined groups (e.g., Cant, 1981; Smith and Rhode, 1989). One group receives the majority of auditory-nerve input via their dendrites and another group receives primary input via their somata. It is hypothesized that the responses of the first group will be regular as significant dendritic (low-pass) filtering of the auditory-nerve input will provide a smooth input current profile to the cell, which produces regular output. The theory further predicts that if the majority of AN-fibers converge on the somata of cells, the low-pass filtering effect is by-passed and the input to the cell remains irregular. In this case, the irregularity of the auditory-nerve input largely determines the irregularity of the output. The viability of this theory rests upon the supposition that significant dendritic filtering is imposed on the auditory-nerve signal as it travels from dendrite to soma. To date, however, this does not seem to be the case, although the evidence is indirect. Smith and Rhode (1989) have shown that the majority of auditory-nerve fibers to sustained choppers synapse very close (within 100 μm) of the cell soma, which may give very limited scope for significant low-pass filtering. The implication is, that the regular/irregular response dichotomy is not due to the degree of dendritic filtering.

IV. CONCLUSIONS

A model of a cochlear nucleus stellate cell has been used to generate hypotheses concerning the generation of different chopper response patterns. The transience of the initial chopping pattern was sensitive to a number of independently varied parameters (cell firing threshold, number of auditory-nerve inputs, and current input strength). A transient chopper response pattern could be generated from the model without the need for the activation of inhibitory inputs. The work complements that of Banks and Sachs (1991) and Arle and Kim (1991) who suggest that the transient chopper response pattern results from an varying input profile as demonstrated here. Two major influences may contribute to the response namely inhibition and auditory nerve adaptation. The type of response pattern observed may be due to intercell differences such as cell firing threshold.

ACKNOWLEDGMENTS

This work was supported by SERC, U.K. and an equipment grant from Apple Computers Inc., U.S.A. We thank the two anonymous reviewers who provided helpful comments on an earlier version of this paper.

APPENDIX: MODEL STAGE 7: STELLATE CELL MEMBRANE MODEL (MACGREGOR, 1987, POINT NEURON 10, p. 458)

The model is activated by a single input function which represents the stimulating current from an experimentally applied electrode. The model is characterized by four variables.

- (1) The transmembrane potential measured as a deviation from the cell resting potential.
- (2) A potassium conductance.
- (3) The time-varying threshold.
- (4) An all-or-nothing spiking variable. Changes in these variables are governed by four differential equations. The first describes the change in the transmembrane potential in response to input current:

$$\frac{dE(t)}{dt} = \frac{(-E(t) + \{[I(t)/G] + G_k(t)/G \cdot [E_k - E(t)]\})}{\tau_m}, \quad (\text{A1})$$

where $E(t)$ is the instantaneous cell-membrane potential above resting level E_R ; $E(0)=0$; $G_k(t)$ is the instantaneous cell potassium conductance $G_k(0)=0$; G is the total resting conductance of soma; τ_m is the membrane time constant; E_k is the equilibrium potential of potassium conductance relative to cell resting level; and $I(t)$ is the current at the soma.

The equation describing the change in potassium conductance is as follows:

$$\frac{dG_k(t)}{dt} = \frac{[-G_k(t) + (b \cdot s)]}{\tau_{Gk}}, \quad (\text{A2})$$

where b is the delayed rectifier potassium conductance strength; s is the spiking variable (0 or 1); $s=0$ if $E(t) < \text{Th}(t) - 1$ if $E(t) \geq \text{Th}(t)$; and τ_{Gk} is the time constant of potassium conductance decay.

G_k rises following an action potential but, otherwise, is continually reducing to zero. The model includes a term for accommodation whereby a cell's firing threshold varies as a function of stimulation. The equation describing the change in threshold is as follows:

$$\frac{d\text{Th}(t)}{dt} = \frac{\{-[\text{Th}(t) - \text{Th}_0] + c \cdot E(t)\}}{\tau_{\text{Th}}}, \quad (\text{A3})$$

where $\text{Th}(t)$ is the time-varying threshold of the cell, Th_0 is the resting threshold of the cell, c is the accommodation constant, and τ_{Th} is the time constant of threshold.

The main output function $p(t)$ is a combination of the transmembrane potential and the spiking variable and represents the record that would be measured with an intracellular microelectrode:

$$p(t) = E(t) + s[E_b - E(t)], \quad (\text{A4})$$

where E_b is the constant representing spike height, s is the spiking variable (see above). A spike is counted when $s=1$.

¹For a Poisson process we expect $\text{CV}=1$ (Papoulis, 1965). Where a minimum interspike interval is introduced (e.g., a refractory period), we expect

$$\text{CV} = 1 - t_D/\mu_R,$$

where t_D is the minimum interval. When the unit is firing perfectly regularly at its maximum rate, $t_D=\mu_R$ and CV has an expected value of zero.

The CV statistic has the virtue of correcting interspike interval variance for firing rate but it should be noted that this correction is not perfect and different firing rates do result in different expected CV values.

- ²The values of the parameters N and ΔI were selected such that the resulting current delivered to the model cell-soma over a 50-ms tone burst never averaged more than 1 nA. This is congruent with examples from the literature where current pulses are injected in to stellate cell soma maintained *in vitro* (e.g., Oertel *et al.*, 1988).
- Arle, J. E., and Kim, D. O. (1991). "Neural modeling of intrinsic and spike-discharge properties of cochlear nucleus neurons," *Biol. Cyber.* **64**, 273–283.
- Banks, M. I., and Sachs, M. B. (1991). "Regularity analysis in a compartmental model of chopper units in the anteroventral cochlear nucleus," *J. Neurophysiol.* **65**, 606–629.
- Blackburn, C. C., and Sachs, M. B. (1989). "Classification of unit types in the anteroventral cochlear nucleus: PST histograms and regularity analysis," *J. Neurophysiol.* **62**, 1303–1329.
- Blackburn, C. C., and Sachs, M. B. (1990). "The representation of the steady-state vowel sound /e/ in the discharge patterns of cat anteroventral cochlear nucleus neurons," *J. Neurophysiol.* **63**, 1191–1212.
- Cant, N. B. (1981). "The fine structure of two types of stellate cells in the anterior division of the anteroventral cochlear nucleus of the cat," *Neuroscience* **6**, 2643–2655.
- Cant, N. B., and Morest, D. K. (1984). "The structural basis for stimulus coding in the cochlear nucleus of the cat," in *Hearing Science, Recent Advances*, edited by C. I. Berlin (College Hill, San Diego), pp. 371–421.
- Hastings, N. A. J., and Peacock, J. B. (1975). *Statistical Distributions* (Butterworths, London).
- Hewitt, M. J., and Meddis, R. (1991). "An evaluation of eight computer models of mammalian inner hair-cell function," *J. Acoust. Soc. Am.* **90**, 904–917.
- Hewitt, M. J., Meddis, R., and Shackleton, T. M. (1992). "A computer model of a cochlear nucleus cell: Responses to pure-tone and amplitude-modulated stimuli," *J. Acoust. Soc. Am.* **91**, 2096–2109.
- MacGregor, R. J. (1987). *Neural and Brain Modeling* (Academic, San Diego).
- Meddis, R. (1986). "Simulation of mechanical to neural transduction in the auditory receptor," *J. Acoust. Soc. Am.* **79**, 702–711.
- Meddis, R. (1988). "Simulation of auditory-neural transduction: Further studies," *J. Acoust. Soc. Am.* **83**, 1056–1063.
- Meddis, R., and Hewitt, M. J. (1991). "Virtual pitch and phase sensitivity of a computer model of the auditory periphery: I. Pitch identification," *J. Acoust. Soc. Am.* **89**, 2866–2882.
- Meddis, R., Hewitt, M. J., and Shackleton, T. M. (1990). "Implementation details of a computational model of the inner hair-cell/auditory-nerve synapse," *J. Acoust. Soc. Am.* **87**, 1813–1816.
- Oertel, D. (1985). "Use of brain slices in the study of the auditory system: spatial and temporal summation of synaptic inputs in cells in the anteroventral cochlear nucleus of the mouse," *J. Acoust. Soc. Am.* **78**, 328–333.
- Oertel, D., Wu, S. H., and Hirsch, J. A. (1988). "Electrical characteristics of cells and neuronal circuitry in the cochlear nuclei studied with intracellular recordings from brain slices," in *Auditory Function*, edited by G. M. Edelman, W. E. Gall, and W. M. Cowan (Wiley, New York), pp. 313–336.
- Papoulis, A. (1965). *Probability, Random Variables and Stochastic Processes* (McGraw-Hill, New York).
- Patterson, R. D., Nimmo-Smith, I., Holdsworth, J., and Rice, P. (1988). "Spiral vos final report, Part A: The auditory filterbank," Cambridge Electronic Design. Contract Rep. APU 2341.
- Pfeiffer, R. R. (1966). "Classification of response pattern of spike discharges for units in the cochlear nucleus: Tone burst stimulation," *Exp. Brain Res.* **1**, 220–235.
- Rall, W. (1989). "Cable theory for dendritic neurons," in *Methods in Neuronal Modeling: From Synapses to Networks*, edited by C. Koch and I. Segev (MIT, Cambridge, MA), pp. 9–62.
- Rhode, W. S., and Greenberg, S. (1992). "Physiology of the cochlear nuclei," in *The Mammalian Auditory Pathway: Neurophysiology*, edited by A. N. Popper and R. R. Fay (Springer-Verlag, Berlin), pp. 94–152.
- Rhode, W. S., Oertel, D., and Smith, P. H. (1983). "Physiological response properties of cells labeled intracellularly with horseradish peroxidase in the cat ventral cochlear nucleus," *J. Comp. Neurol.* **213**, 448–463.
- Romand, R. (1978). "Survey of intracellular recording in the cochlear nucleus of the cat," *Brain. Res.* **148**, 43–65.
- Romand, R. (1979). "Intracellular recordings of chopper responses in the cochlear nucleus of the cat," *Hear. Res.* **1**, 95–99.
- Rouiller, E. M., and Ryugo, D. K. (1984). "Intracellular marking of physiologically characterized cells in the ventral cochlear nucleus of the cat," *J. Comp. Neurol.* **225**, 167–186.
- Smith, P. H., and Rhode, W. S. (1989). "Structural and functional properties distinguish two types of multipolar cells in the ventral cochlear nucleus," *J. Comp. Neurol.* **282**, 595–616.
- Westerman, L. A., and Smith, R. L. (1984). "Rapid and short-term adaptation in auditory nerve responses," *Hear. Res.* **15**, 249–260.
- Young, E. D., and Barta, P. E. (1986). "Rate responses of auditory nerve fibers to tones in noise near masked threshold," *J. Acoust. Soc. Am.* **79**, 426–442.
- Young, E. D., Robert, J.-M., and Shofner, W. P. (1988a). "Regularity and latency of units in the ventral cochlear nucleus: Implications for unit classification and generation of response properties," *J. Neurophysiol.* **60**, 1–29.
- Young, E. D., Shofner, W. P., White, J. A., Robert, J.-M., and Voigt, H. F. (1988b). "Response properties of cochlear nucleus neurones in relationship to physiological mechanisms," in *Auditory Function*, edited by G. M. Edelman, W. E. Gall, and W. M. Cowan (Wiley, New York), pp. 277–312.